

## SAR-DiskSat for Mega-Constellation

Hirobumi Saito

Waseda University, Faculty of Science and Engineering, 3-4-1 Okubo, Shinjyuku-ku, Tokyo, 169-8555 Japan,  
saito.hirobumi@aoni.waseda.jp

Mitsuteru Kaneoka

CSP Japan 2-16-1 Kyobashi, Chuo-ku, Tokyo, 104-0031 Japan, kaneoka@csp.co.jp

Richard P. Welle and Anastasia Muszynski

The Aerospace Corporation, PO Box 92957, Los Angeles, CA, USA, 90009, welle@aero.org

### ABSTRACT

We have developed and demonstrated in 2021 small SAR satellites of 1-m ground resolution with novel deployable slot array antennas. This paper newly proposes a novel concept of quasi-two-dimensional SAR satellites, SAR-DiskSats with this deployable passive slot array antenna. The deployable slot array antennas can be compactly folded in the quasi-two-dimensional satellite body. Also, it is possible to install flexible solar cell sheets on the back side of the antenna because the antennas do not dissipate heat. This quasi-two-dimensional satellite configuration is suitable for stacking in a rocket faring for mega-constellation launching. Another advantage of the SAR-DiskSat is the possibility of VLEO (very low Earth orbit) operation. A thin edge cross-section makes aero drag small and there is an advantage of short range in terms of signal-to-noise ratio. This advantage of RF power makes it easier to improve its ground resolution. We are developing a new corporate feed slot array antenna with very wide-band (1.2-GHz bandwidth in X band) for 0.25-m ground resolution. The final goal of this SAR-DiskSat would be a mega-constellation of 0.25-m ground resolution in VLEO.

### INTRODUCTION

Synthetic Aperture Radar (SAR) has several benefits for remote sensing applications compared with optical imagery like uninterrupted image acquisition even at night or during cloud cover. However, conventional SAR observation requires large or medium size satellites weighing several hundred kilograms.

With rapid advancements in miniaturization of space technology, SAR sensors on board micro-satellites in LEO is becoming quite popular both for research and commercial applications. Capella Space<sup>1</sup> and Iceye<sup>2</sup> are contemporary examples of the small SAR satellites.

Also, the authors' group have developed a small SAR sensor, Micro-X-SAR<sup>3</sup> with a unique deployable slot array antenna. The SAR system has been successfully demonstrated in orbit by Strix- $\alpha$  satellite<sup>4</sup> of Synspec Inc. in Feb. 2021. Three SAR satellites are in orbit as of Nov. 2022. These groups plan to have their own SAR satellite constellation which consists of several tens of SAR satellites. Their SAR satellites are almost cubic in shape and one to several satellites are launched simultaneously by a small rocket.

An emerging trend of small satellite missions is a mega-constellation, which consists of hundreds or thousands of satellites to make revisit time shorter and shorter. Starlink has already launched over three thousand communication small satellites. One large rocket launches sixty satellites simultaneously.

In 2021, Aerospace Corporation proposed a DiskSat<sup>5,6</sup>, a containerized, large aperture, quasi-two-dimensional satellite bus architecture. The concept of DiskSat is evolved from CubeSats. In the past decade the cumulative number of CubeSats flown has increased from well under 100 to well over 1000. However, with the growth of commercial applications of CubeSats, often requiring more payload volume or power, interest in larger CubeSats is accelerated.

A representative DiskSat structure is a composite flat panel, one meter in diameter and 2.5 or 5 cm thick, to which components are affixed in a flat pattern within the panel. For launch, multiple DiskSats are stacked in a fully enclosed container/dispenser using a simple mechanical interface, and are released individually once in orbit. Stacking of 20 or more DiskSats is possible in

small launch vehicles, making it ideal for building large constellations of small satellites (mega-constellation).

Another feature is the ability to fly in a low-drag orientation which, in combination with electric propulsion for drag makeup, enables flight at very low altitudes in LEO (VLEO). This feature of DiskSat is very attractive for SAR applications since the signal-to-noise ratio of SAR images is inversely proportional to cube of the altitude.

The SAR antennas of the authors' group are very suitable for SAR-DiskSat missions since they have low costs, thin shapes, both at stowed condition in a rocket faring and after deployment, unlike other types of SAR antennas, active-phased-array antennas, and deployable mesh antennas. The Aerospace Corporation is developing a demonstration DiskSat mission with satellites of one meter diameter, having about 12 kg mass and about 160 W of power generation. These resources seem small for SAR missions. However, one of the DiskSat guiding principles is that the design approach should be adaptable to various diameters and various thicknesses.

This paper describes a summary of the present small SAR satellites with cubic shapes, a new concept of SAR-DiskSat, performance evaluation of SAR-DiskSat, operation in VLEO, and present status of very wideband slot array antennas development.

### SUMMARY OF MICRO-X-SAR

This section describes our 100-kg-class SAR satellite, Micro-X-SAR, three models of which have already flown<sup>3,4</sup>. From considerations of low-cost, lightweight, and simple fabrication for mass production, a passive honeycomb panel slot-array antenna with waveguide feeder network system was selected. As described later, this slot-array antenna is a series feed antenna for medium ground resolution.

Fig. 1 is a photograph of the Micro-X-Sar with the deployed SAR antenna. There are flexible solar sheets



Fig. 1. Outlook of Micro-X-SAR satellite with solar cell sheets on back side of deployed antenna panels.

on the back side of the SAR antenna. Each panel is 70 cm x 70 cm in size and the antenna size in deployed condition is 5 m x 0.7 m. The stowed condition at launch can be fit into a 0.7 m x 0.7 m x 0.7 m satellite body. The waveguide is embedded at the rear antenna surface in order to feed RF to the antenna panel through coupling slots. The antenna panel consists of a dielectric honeycomb core and metal skins, which function as a parallel plate guide for radio wave signal. The front surface with two-dimensional arrays of radiation slots works as an antenna radiator for vertical polarization SAR mode. After the SAR antenna is deployed, RF power is fed between adjacent panels through a contactless choke flange with a nominal airgap of 0.9 mm.

Fig. 2 is the layout of Micro-X-SAR satellite as of 2018<sup>7</sup>. The satellite body for all instruments except for the SAR

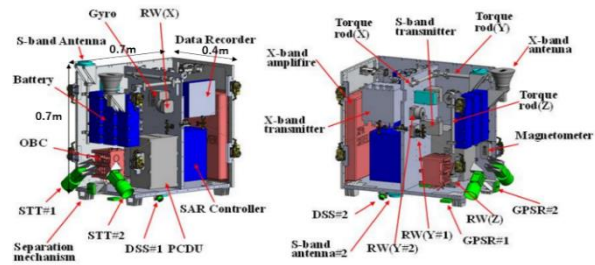


Fig. 2. Layout of First-Generation Micro-X-SAR. Satellite<sup>7</sup>. Body Size 0.7 x 0.7 x 0.4 m.

Table 1. Specification of Micro-X-SAR

Item	SAR Mode	
	Strip Map	Sliding Spotlight
Altitude	600km	
Resolution	3m	1m
Center Frequency	9.65GHz	
Swath	25 km	25km
Chirp Band Width	75MHz	300MHz
Polarization	V/V	
Antenna Size	4.9 m×0.7 m	
Ant Efficiency	50%	
TX Peak Power	1000 W	
TX Duty	25%	
System Loss	0.6 dB	
System Noise Figure	2.6 dB	
Off Nadir Angle	15~45 deg	
Pulse Repetition Frequency	3000 ~ 8000 Hz	
NESZ (beam center)	-15dB	-18dB
Ambiguity (beam center)	>15dB	

antenna is  $0.7 \text{ m} \times 0.7 \text{ m} \times 0.4 \text{ m} = 0.2 \text{ m}^3$ . Note that the PCDU (power control and distribution unit) the battery (BAT) and the SAR Controller (SELU) have large volume. Since the X-band high-power amplifier/transmitter (XPA) requires a large area for thermal radiation, XPA is flat in shape (45 cm x 45 cm x 5 cm) and is integrated on the satellite body panel.

The SAR system specification of Micro-X-SAR is shown in Table 1.

### CONCEPT of SAR-DISKSAT

The unique feature of Micro-X-SAR satellite the deployable passive slot array antenna. The antenna system consists of flat passive slot array antenna panels with thickness of about 4 cm per one panel. The stowed configuration of the antenna is also compact since the panel shape is flat. Since all active devices are inside the satellite body, there is no heat dissipation in the antenna. It is possible to install solar cells as shown in Fig. 1. Particularly in Micro-X-SAR a combination of flexible solar cell sheets and multi-layer-insulator films are applied to avoid antenna thermal distortion. Consequently, the shape of SAR satellites with the deployable passive slot array antenna can be very simple and thin both in the launching phase and in the orbit phase. It seems this type of SAR satellites are the most suitable to DiskSats, quasi-two-dimensional satellites.

This feature of SAR-DiskSat contrasts with SAR satellites having other types of SAR antennas such as deployable mesh parabolic antennas or active-phased-array antennas. The former require a deployable main dish, sub-dish, and solar panels, which cannot be flat either at launch or in flight. The latter have flat antenna panels with a certain thickness and heat dissipation. They need an independent deployable solar panel.

Fig. 3 is a conceptual configuration of a SAR-DiskSat with four antenna panels. The upper is the shape before antenna deployment, which is  $1 \text{ m} \times 1 \text{ m} \times 0.25 \text{ m}$  and can be vertically stacked in a launcher fairing as shown in Fig. 4. This launching configuration is very suitable to a SAR mega-constellation. The lower of Fig. 3 is the shape after antenna deployment. The front is the radiation surface and there are flexible solar sheets and multi-layer thermal insulators on the rear surface. Approximately 400 W dc power can be generated by the four panels.

The thickness of one antenna panel is 4 cm, which is determined by the shape of the groove in the waveguide choke flanges. It is reasonably assumed that the thickness of the stowed four-panel antenna is 0.2 m. The DiskSat body, which fits in an envelope of  $1 \text{ m} \times 1 \text{ m} \times 0.25 \text{ m}$  during launch includes a cutout of  $0.75 \text{ m} \times 0.75 \text{ m} \times 0.2 \text{ m}$  to stow the SAR antenna. The volume

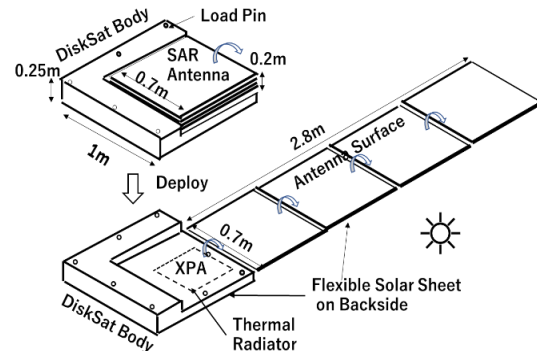


Fig. 3. Conceptual Configuration of SAR-DiskSat with 1m Square. Antenna panel number may increase for higher resolution and power.

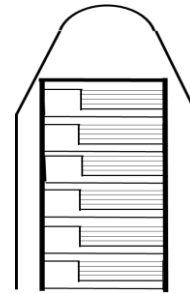


Fig. 4. Launch configuration of SAR-DiskSat

available for all satellite instruments except for the antenna is  $1 \text{ m} \times 1 \text{ m} \times 0.25 \text{ m} - 0.75 \text{ m} \times 0.75 \text{ m} \times 0.2 \text{ m} = 0.14 \text{ m}^3$ .

As shown in the previous chapter, for the present small SAR satellite Micro-X-SAR, the volume for satellite instruments is  $0.2 \text{ m}^3$ . It seems possible to reduce volume of instruments of DiskSat SAR by  $0.06 \text{ m}^3$  or 30% from the present Micro-X-SAR. The strategy for volume reduction is (i) to replace the traditional bus instruments by recent CubeSat instruments, (ii) volume reduction of SAR Electronics Unit, (iii) volume reduction of batteries and power control unit.

The present X band power amplifier (XPA) is  $45 \text{ cm} \times 45 \text{ cm} \times 5 \text{ cm}$  in size and can be installed near the antenna as shown in Fig. 3. The downward direction is sun facing. Therefore, there are thermal radiators on the upward surface.

### PERFORMANCE of SAR-DISKSAT

DiskSat has the potential to utilize very low Earth orbit (VLEO), which can contribute to compact SAR satellite.

This section describes possible DiskSat SAR performances. The signal-to-noise-ratio  $SNR_{image}$  of the SAR image is given by Cutrona<sup>8</sup>.

$$SNR_{image} = \frac{P_{ave} A^2 \eta^2 \delta_r \sigma^0}{8\pi R^3 kT NF v \lambda L_s} \quad (1)$$

where  $k$  is the Boltzman's constant, and  $T$  is the noise temperature of the receiving system.  $R$  is a slant range between the satellite and the surface target.  $A$ , and  $\eta$  are a SAR antenna aperture area, and an aperture efficiency of the SAR antenna.  $\sigma^0$  is the normalized radar cross section per a unit area and  $\delta_r$  are range resolutions, respectively.  $\lambda$  is the wavelength.  $L_s$  is a system loss. A received power of primary radars is proportional to  $A^2/R^4$ . However, the synthetic aperture effect has a time integration effect which is proportional to  $R$ . Then the signal-to-noise ratio of SAR images is proportional to  $A^2/R^3$ . This means that a required antenna area is proportional to  $(R^3/\delta_r)^{1/2}$  for a given  $SNR_{image}$ .

Micro-X-SAR, a conventional SAR satellite, has seven antenna panels in LEO (600 km altitude) as shown in Fig. 1 and the highest SAR performance is 1-m ground resolution (Table 1). The performance of SAR-DiskSat can be estimated based on the simple scaling (1).

Table 2 shows the estimated SAR performances of SAR-DiskSat, where the signal-to-noise ratios are evaluated.  $P_t$  is the peak transmitting power with on-duty 25% and  $\delta_r$  is the range resolution. The ground resolution of DiskSat with four antenna panels and 1 kW peak power is 3 m for 600 km altitude LEO. If SAR-DiskSat is in VLEO (350 km altitude), then the signal-to-noise ratio increases by a factor  $(600/350)^3=5$  for a constant antenna panel number and ground resolution. If the signal-to-noise ratio is kept constant, the ground resolution can be improved by a factor 5. The ground resolution of SAR-DiskSat with four and seven panels are 0.6 m and 0.2 m, respectively. This result is an extremely attractive merit to realize a compact SAR-DiskSat.

Fig. 5 shows the ground resolution as a function of the altitude (horizontal axis) and the antenna panel number (vertical axis, left). The ground resolution improves as

Table 2. Ground Resolution of SAR-DiskSat

	1st Gen. Micro-X-SAR(2018)		DiskSat LEO			DiskSat VLEO 350km	
	Res3m	Res1m	Res3m	Res1m	Res0.3m	Res0.6m	0.2m
Panel#	7	7	4	7	7	4	7
BW(MHz)	75	300	75	300	1000	500	1500
Pt(kW)	1	1	1	1	3	1	1
Alt(km)	600	600	600	600	600	350	350
$\delta_r$ (m)	3	1	3	1	0.3	0.6	0.2

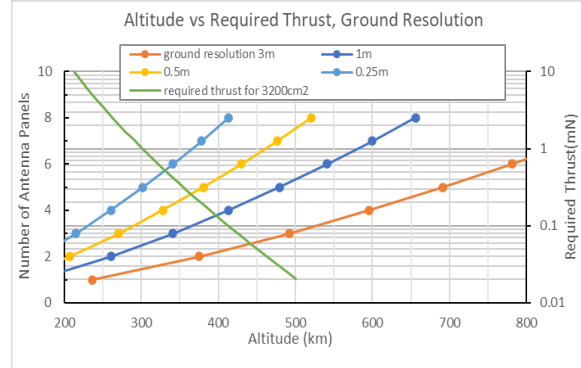


Fig. 5. Altitude vs. Required Thrust and Ground Resolution assuming 1 kW peak power and 25% duty cycle.

the altitude decreases and as the antenna panel number increases.

### Operation in VLEO

Although yet to be demonstrated in flight, an analysis by the Aerospace Corporation in 2022 indicated that a DiskSat with an edge area of 322 cm<sup>2</sup> should be able to maintain an orbit of 250 km altitude (VLEO) with 0.35 mN thrust, based on the NRL MSISE00 atmosphere model<sup>6</sup>. This thrust level can be generated by various small electric thrusters such as, for example, the Expulsion Nano FEPP (field emission electric propulsion). The power consumption of this thruster is 40 W, and the size is 10 cm x 10 cm x 10 cm.

As shown in the previous section, the edge area of the proposed SAR-DiskSat is typically 100 cm x 25 cm = 2500 cm<sup>2</sup>, which is an order magnitude larger than the above value. Fortunately, the NRL MSISE00 model describes that atmospheric density at 350 km is typically an order magnitude smaller than at 250 km. Thus, one may expect to maintain an orbit of 350 km altitude using a thruster capable of continuous operation at 0.35 mN thrust.

However, very low Earth orbits present a highly dynamic mission environment, and it is necessary to undertake a more detailed analysis considering atmospheric variability. The perturbation most greatly affecting satellites at 350 km altitude is atmospheric drag, which will depend on the vehicle cross-sectional area, the orientation of the vehicle in flight, and the atmospheric density. Atmospheric density in VLEO is highly variable and heavily influenced by the solar cycle. To evaluate propulsion requirements, the atmosphere is modeled with the MSISE00 atmospheric model, which considers the predicted geomagnetic index, and the 10.7-cm solar radio flux index. This consideration is particularly important since a launch window in 2024-2026 will

coincide with a solar maximum, resulting in increased atmospheric densities. Historical atmospheric data shows that daily spikes in geomagnetic activity and solar flux are both possible and expected during a solar maximum. The results below are modeled with the expected 50<sup>th</sup> percentile and 95<sup>th</sup> percentile atmospheric densities, which reflect expected variations over the course of a month, as well as an expected worst-case daily spike during a solar maximum.

In translating these atmospheric density variations into propulsion requirements, it is useful to think in terms of duty cycle; electric thrusters are typically capable of producing a continuous or near-continuous low thrust, which is ideal for drag makeup when trying to maintain a constant altitude. Because the atmospheric density is not constant, the average thrust required to maintain orbit will vary, and this is accomplished by operating the thruster with a duty cycle that will produce the required average thrust. Table 3 lists the expected duty cycle required to maintain orbit under three different atmospheric conditions assuming a thruster capable of providing 0.35 mN at the required duty cycle. Also considered is the spacecraft attitude. For the reference design under ideal attitude control, the cross-sectional area is 2500 cm<sup>2</sup>. However, if the vehicle attitude drifts from ideal, the effective cross-sectional area increases, reaching 3273 cm<sup>2</sup> at an offset of 1.5 degrees from ideal.

As shown in Table 3, under typical atmospheric conditions the duty cycle required to maintain altitude is between 20% and 30% depending on the accuracy of the attitude-control system. Even with a 95% atmosphere, the thruster duty cycle does not exceed 60%. It is possible, however, for the atmospheric density to spike briefly due to solar activity. Under the worst-case daily spike, the duty cycle required to maintain altitude with ideal attitude control reaches over 90%. With a 1.5 degree offset from ideal attitude, the required thruster duty cycle exceeds 100%. Since it is impossible to operate a thruster more than 100% of the time, the impact of this is that the satellite would lose altitude for as long as the atmospheric density remains high. While loss of altitude is not ideal, the problem would be temporary; according to historical data, these worst-case spikes generally pass within a day, and SAR-DiskSat should be able to recover to 350 km altitude once more favorable atmospheric conditions return. It is important, however, that the vehicle be able to thrust continuously, even when in eclipse, to maintain a circular orbit, which should be taken into consideration when designing the power subsystem.

In recovering from a worst-case atmosphere spike, the SAR-DiskSat will have lost some altitude, and the atmospheric density will be higher than at 350 km.

Assuming the spike lasts no more than a day or two, the altitude loss will be no more than a few km, and recovery should take no more than a few days. On the other hand, if a satellite gets low enough, then it will eventually become impossible to recover. The minimum recoverable altitude is the lowest altitude at which the thrust provided from the propulsion unit operating at 100% duty cycle can overcome drag and raise the orbit. This is shown for various atmospheric conditions and two attitude orientations in Table 4.

Table 3. Required Thrust Duty Cycle to Maintain 350 km Altitude for Various Atmospheric Parameters, Launch: Jan 2025, MSIS00 Atmospheric Model.

Atmospheric Condition	Edge-On Attitude	1.5° Attitude Offset
50 <sup>th</sup> Percentile	21%	28%
95 <sup>th</sup> Percentile	45%	60%
Worst-Case Daily Spike	91%	104% *

\*Duty cycle greater than 100% indicates thrust level not sufficient to maintain altitude with this attitude and these atmospheric conditions

Table 4. Minimum Recoverable Altitude for Various Atmospheric Parameters, Launch: Jan 2025, MSIS00 Atmospheric Model.

Atmospheric Condition	Edge-On Attitude	1.5° Attitude Offset
50 <sup>th</sup> Percentile	300 km	315 km
95 <sup>th</sup> Percentile	340 km	350 km
Worst-Case Daily Spike	370 km	385 km

It is expected that the attitude control system for the SAR-DiskSat should easily be able to maintain an attitude well within 1.5 degrees, and altitude loss due to atmospheric drag should remain within acceptable limits. Should attitude control be lost altogether the vehicle may begin to tumble, in which case the rate of altitude loss would drastically increase. During nominal operations, however, the SAR-DiskSat would be flown close to edge-on, with the satellite body ahead of the deployable panels as shown in Fig.6. It should be noted that in this configuration a small electric thruster is attached at the tip of the deployable panels. When flying in this

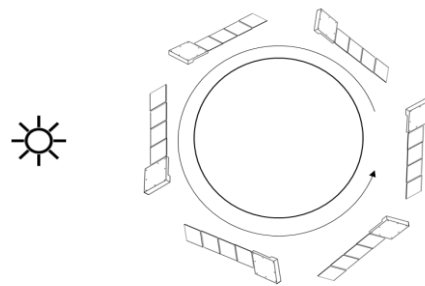


Fig. 6. SAR-DiskSat Operation in VLEO.

configuration the center of mass would remain ahead of the center of pressure, and thus even without active attitude control the vehicle should be aerodynamically stable and at low risk of entering a tumble due to drag effects. Thus, an electric thruster with 0.35 mN continuous thrust capability should be sufficient to ensure safe operation of SAR-DiskSat at 350 km altitude.

In conventional LEO at altitudes between 500 and 600 km, atmospheric density is less than 1% of the density at 250 km so atmospheric drag is low. Solar panels may be directed toward the sun to produce peak power; the SAR-DiskSat with four antenna panels would produce a peak power of about 400 W and the average power is about 1/2 of the peak power due to eclipse.

However, in VLEO the antenna/solar panels should be oriented to minimize atmospheric drag. As shown in Fig. 6, the lowest drag is achieved when the velocity vector is parallel to the long axis of the satellite when the panels are unfolded. From a drag perspective, the satellite is free to rotate about this "roll" axis as necessary to produce peak solar power. In a noon/midnight polar orbit at VLEO, the solar panels ideally point toward zenith and the orbit-average power is about  $1/\pi$  times the peak power. To maintain adequate power, it may be necessary to increase antenna/solar panel number. When the local time of the polar orbit moves away from a noon/midnight orbit, the orbit-average power can be increased by rotating the satellite about the roll axis to point the solar arrays toward the sun. Ultimately, in a dusk/dawn orbit, the peak power can be generated throughout the orbit by rotating the satellite 90 degrees about its roll axis. It should be noted that the antenna normal direction is directed to a target point on ground in SAR observation duration, which is typically several minutes.

## VERY WIDE BANDWIDTH SLOT ARRAY ANTENNA

From microwave to millimeter-wave, planar slot waveguide antennas have been one of the most attractive categories due to advantages of high efficiency, compact geometry, easy-to-control aperture distribution and simple installation.

In planar arrays, slots are usually etched serially on the walls of hollow rectangular waveguides. Proper modes should be excited and fed to slotted parts in these waveguides to finally create a radiation into the free space.

As described in the previous chapter, SAR observations in VLEO with quasi-2D satellites have a significant advantage in terms of signal-to-noise ratio. Eq. (1) shows that the signal-to-noise ratio is proportional to both  $R^{-3}$

and  $\delta_r$ . This means that SAR observations in VLEO give us a chance to improve ground resolution if the chirp frequency band can be widened enough for the ground resolution. The present Micro-X-SAR has the chirp bandwidth of 300 MHz for 1-m ground resolution. As a next step, the authors are developing a planar slot-array antenna with 1.2-GHz bandwidth in X band for 0.25-m ground resolution.

Main schemes to feed radio wave to radiation slots are series feed and corporate (or parallel) feed. The

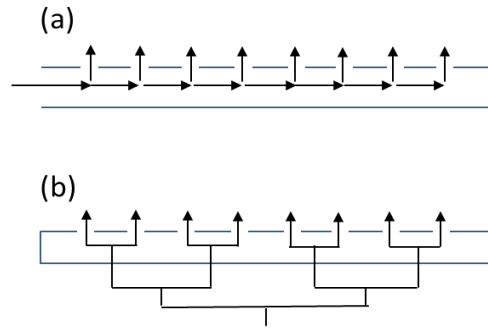


Fig. 7. (a) Series Feed Slot Array Antenna. (b) Corporate Feed (Parallel Feed) Slot Array Antenna.

configuration of series feed is shown in Fig. 7(a), where each slot is excited in series by a travelling wave or a standing wave in a waveguide. The slot spacing can be adjusted so that radiation from each slot is in-phase at the center frequency. However, radiation phase distribution deviates from in-phase as frequency shifts from the center frequency, resulting in performance degradation. Practical bandwidth of a series feed antenna is less than  $1/(2N)$  where  $N$  is a total number of slots in series. An example of antenna bandwidth with series feed is less than 7% bandwidth for  $N=7$ . In X band SAR application, 600-MHz bandwidth is possible to realize 0.5-m ground resolution. Merits of the series feeds are shorter path leading to less loss and relatively simple structures. For the sake of this simplicity, the present Micro-X-SAR has the chirp bandwidth of 300 MHz for 1-m ground resolution.

The configuration of corporate feed (parallel feed) is shown in Fig. 7(b), where the feeder circuit consists of a tournament circuit. Electrical length of feeder to each slot is equal and in-phase excitation can be maintained in a wide bandwidth. The corporate feeds feature wide bandwidth at the expense of complicated configuration. Recently, high ground resolution of 0.25 m is discussed for SAR observation assuming 1.2-GHz chirp bandwidth in X band. This application may require the corporate feed plane slot array antenna.

In 2022, the authors developed the first bread-board model of X band corporate slot array antenna<sup>9</sup> aiming at very wide bandwidth SAR, based on the 60-GHz corporate feed slot array antenna<sup>10</sup>. The measured reflectivity is less than -15 dB for 9.0-10.2 GHz and the measured aperture efficiency is higher than 84% for 9.2-10.4 GHz. This type of antenna seems very promising for 1.2-GHz bandwidth SAR applications. The remaining issue is to reduce the mass of the antenna.

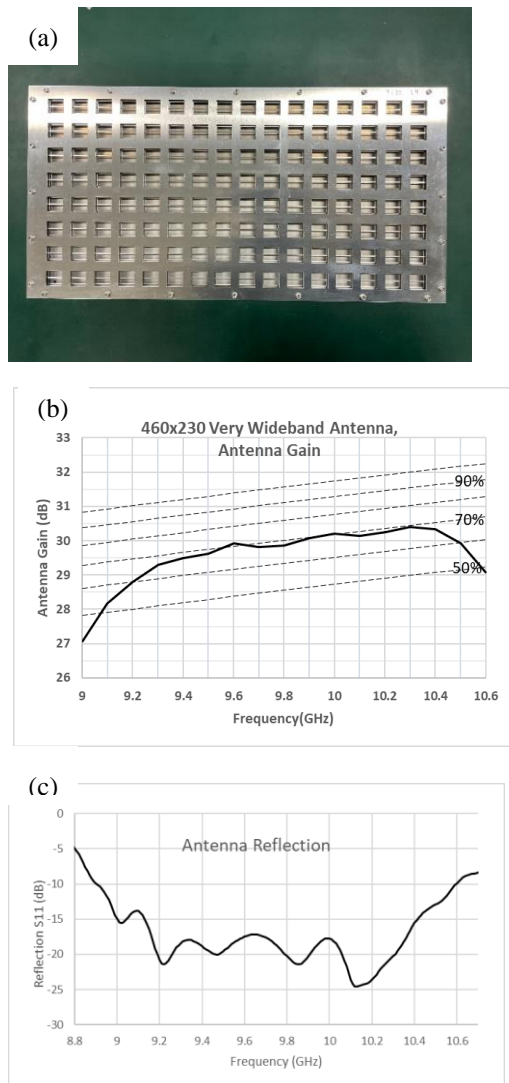


Fig. 8. (a) BBM Model of Very Wide-band Slot Array Antenna (460 x 230 mm). (b) Measured Antenna Gain. (c) Measured Antenna Reflection.

The second bread-board model was manufactured in 2023, paying attention to mass reduction of the antenna. Fig. 8(a) is a photograph of the slot array antenna (46 cm x 23 cm). Fig. 8(b) is the measured antenna efficiency and Fig. 8(c) is the measured reflectivity S11 as a function of frequency. The measured reflectivity is less than -15 dB for 9.2-10.8 GHz and the measured antenna

efficiency is 70% for 9.2-10.4 GHz. We will continue the further developments and apply this type of very wide bandwidth antenna to the SAR-DiskSat illustrated in Fig. 3.

### DEMONSTRATION by SMALL LAUNCHER

The SAR-DiskSat can be in a quasi-2D shape as shown in Fig. 3. This shape may be best fit to a SAR mega-constellation mission, where a large launcher launches several tens of SAR-DiskSats simultaneously. However, the envelop diameter of the satellite configuration of Fig. 3 is about  $\sqrt{2}=1.4$  m.

The first demonstration of the SAR-DiskSat may be single-launched by a small launcher, a faring diameter of which may be about 1 m. A possible configuration of the first SAR-DiskSat demonstration is shown in Fig. 9. All on-board instruments would be installed in the thin cylinder of 1 m diameter and about 0.2 m height. Four or seven antenna panels are folded on the upper deck of the cylinder. One or a few SAR-DiskSats are launched by a small rocket. Then the antenna panels are deployed in orbit and the SAR-DiskSats are in a quasi 2D shape.

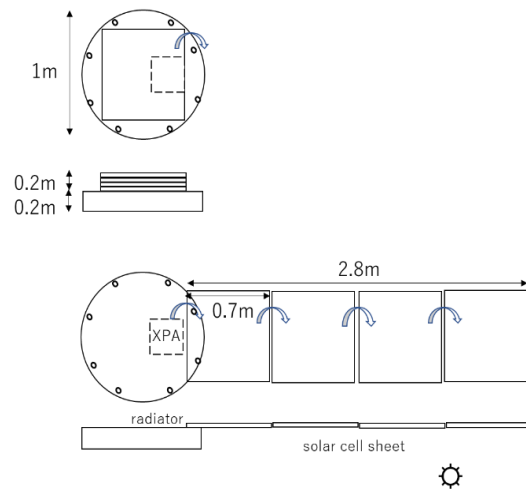


Fig.9. Demonstration of SAR-DiskSat by Small Launcher.

An intensive system design is further necessary including power budget, thermal design, orbit design etc. In parallel the present SAR instruments will be miniaturized to be adapted for a DiskSat.

### Conclusion

This paper proposes a SAR-DiskSat for a coming mega-constellation, in which a low-cost, compactly stowed SAR system with a deployable slot array antenna is applied to the DiskSat architecture. The quasi-two-dimensional SAR-DiskSats can be vertically stacked in

a launcher faring. Another advantage of the SAR-DiskSat is the possibility of VELO operation. The thin shape configuration in orbit makes atmospheric drag small and there is an advantage of short range in terms of signal-to noise ratio. The final goal of the SAR-DiskSat would be a mega-constellation of 0.25-m ground resolution in VLEO.

### Acknowledgments

This research and development work was supported by the MIC/SCOPE #201603001

### References

1. G. Farquharson, W. Woods, C. Stringham, N. Sankarambadi and L. Riggi, "The Capella Synthetic Aperture Radar Constellation," IGARSS 2018 – 2018 IEEE International Geoscience and Remote Sensing Symposium, Valencia, 2018, pp. 1873-1876.
2. O. Antropov, J. Praks, M. Kauppinen, P. Laurila, V. Ignatenko and R. Modrzewski, "Assessment of Operational Microsatellite Based SAR for Earth Observation Applications," 2018 2<sup>nd</sup> URSI Atlantic Radio Science Meeting (AT-RASC), Meloneras, 2018, pp. 1-1.
3. B. Pyne, Hirobumi Saito, Prilando Riziki Akbar, Jiro Hirokawa, Takashi Tomura, and Koji Tanaka, "Development and Performance Evaluation of Small SAR System for 100-kg Class Satellite," "IEEE J. Selected Topics in Appl. Earth Observation and Remote Sensing, vol.13, p.3879, 2020.
4. Krzysztof Orzel, Tomoyuki Imaizumi, Shuji Fujimaru, Motoyuki Arai, and Toshihiro Obata, "The on-orbit demonstration of the small SAR satellite. Initial calibration and observations," 2022 IEEE Radar Conf. March 2022, New York, USA. DOI:10.1109/RadarConf2248738.2022.97642
5. Richard P. Welle, Catherine C. Venturini, David A. Hinkley, Joseph W. Gangestad. "The DiskSat: A Two-Dimensional Containerized Satellite," 35<sup>th</sup> Annual Small Satellite Conference, SSC21-XIII-12, Logan, Utah, USA, Aug. 2021
6. R.Welle, C. Venturini, D.Hinkley, J.Gangestad, S. Grasso, A. Muszynski, R. Hunter, C. Frost, D.Mayer, C.Baker. "DiskSat: Demonstration Mission for a Two-Dimensional Satellite Architecture," Proceedings of the Small Satellite Conference, SSC22-VIII-1, 2022.
7. K.Hirako, S.Shirasaka et al. "Development of Small Satellite for X-Band Compact Synthetic Aperture Radar," 6<sup>th</sup> Int. Seminar of Aerospace Science and Technology. Jakarta, Sep.25-26,2018. J Physics:Conf.Series 1130(2018)012012.L.
8. J. Cutrona, "Synthetic aperture radar," in Radar Handbook, M. I. Skolnik, Ed. New York: McGraw-Hill, 1970, ch. 23, pp. 23.1-23.25.
9. Shuang Ji, Jiro Hirokawa, Takashi Tomura, and Hirobumi Saito, "X-band grating-loaded parallel-plate slot array antenna with low reflection," IEICE Commun. Express, DOI: 10.1587/comex.2023SPL0019, March 2023.
10. Shuang Ji, Jiro Hirokawa, and Takashi Tomura, "A Wideband and High-Gain All-Metallic Perpendicular-Corporate-Fed Multi-Layered Parallel-Plate Slot Array Antenna," IEEE Multidisciplinary Open Access Journal, vol.10,pp.38000, 2022, Digital Object Identifier 10.1109/ACCESS.2022.316512



